Solutions of the Maxwell viscoelastic equations for displacement and stress distributions within the arterial wall

S. Hodis[1] and M. Zamir[1,2]
[1]*Department of Applied Mathematics, University of Western Ontario, London, Ontario, N6A 5B7, Canada*
[2]*Department of Medical Biophysics, University of Western Ontario, London, Ontario, N6A 5B7, Canada*
(Received 30 January 2008; revised manuscript received 2 May 2008; published 29 August 2008)

Mechanical events within the thickness of the vessel wall caused by pulsatile blood flow are considered, with focus on axial dynamics of the wall, driven by the oscillatory drag force exerted by the fluid on the endothelial layer of the wall. It is shown that the focus on the axial direction makes it possible to derive simplified equations of motion which, combined with a viscoelastic model of the wall material, makes it possible in turn to obtain *solutions in closed form* for the displacement and stress of material elements within the wall. The viscoelastic model allows a study of the dynamics of the wall with different ratios of viscosity to elasticity of the wall material, to mimic changes in the properties of the arterial wall caused by disease or aging. It is found that when the wall is highly viscous the displacements and stresses caused by the flow are confined to a thin layer close to the inner boundary of the wall, while as the wall material becomes less viscous and more rigid the displacements and stresses spread deeper into the thickness of the wall to affect most of its elements.

DOI: 10.1103/PhysRevE.78.021914 PACS number(s): 87.85.em, 87.10.Ca, 87.19.rd

I. INTRODUCTION

Mechanical damage of the arterial wall, resulting from shear forces exerted by the moving fluid in pulsatile blood flow, has long been suspected to play a role in the pathogenesis of vascular disease. However, much of the work so far has focused on only one part of the arterial wall, namely the endothelial layer. This layer is indeed in direct contact with the moving fluid and hence subject to shear forces exerted by the flow, but the consequences of these forces are clearly not limited to only that layer of the arterial wall. Depending on the degree of tethering of the wall and on its viscoelastic properties, the consequences of shear forces at the endothelial layer extend into the entire thickness of the arterial wall. Indeed, using high-resolution ultrasonic scanning, it was shown recently that median layers of the wall show larger longitudinal movements than outer layers [1,2]. Thus there is a distribution of longitudinal shear strain and, accordingly, shear stress within the vessel wall, which has not previously been described.

In this paper we examine these longitudinal stresses and strains by using the displacements and shear forces at the endothelial layer as boundary conditions for solutions of the Maxwell viscoelastic model equations [3] within the entire arterial wall thickness. The vessel wall has a very complex structure, but it has been shown experimentally that the media, the middle layer of the wall, is mainly responsible for the viscoelastic behavior of the wall and it behaves mechanically as a homogeneous material [4–6]. For the purpose of our study and as a first step therefore we consider the wall to consist of a homogeneous viscoelastic material. This is clearly an idealization, but by varying the relative values of elasticity and viscosity we hope to capture some of the pathological conditions of the arterial wall under the effects of disease or aging.

II. GOVERNING EQUATIONS

Using a cylindrical polar coordinate system x, r, θ, with x along the vessel axis, r, θ in the radial and circumferential directions respectively, the equations governing the displacement of a material element of the vessel wall are given by

$$\rho\frac{\partial^2\xi}{\partial t^2}=\frac{\partial\sigma_{xx}}{\partial x}+\frac{\partial\sigma_{rx}}{\partial r}+\frac{\sigma_{rx}}{r}+\frac{1}{r}\frac{\partial\sigma_{\theta x}}{\partial\theta}, \tag{1}$$

$$\rho\frac{\partial^2\eta}{\partial t^2}=\frac{\partial\sigma_{xr}}{\partial x}+\frac{\partial\sigma_{rr}}{\partial r}+\frac{\sigma_{rr}}{r}+\frac{1}{r}\frac{\partial\sigma_{\theta r}}{\partial\theta}-\frac{\sigma_{\theta\theta}}{r}, \tag{2}$$

$$\rho\frac{\partial^2\phi}{\partial t^2}=\frac{\partial\sigma_{x\theta}}{\partial x}+\frac{1}{r^2}\frac{\partial(r^2\sigma_{r\theta})}{\partial r}+\frac{1}{r}\frac{\partial\sigma_{\theta\theta}}{\partial\theta}, \tag{3}$$

where ξ, η, ϕ are displacements in the x, r, θ directions, respectively, σ_{ij} $(i,j=x,r,\theta)$ are elements of the stress tensor, and t is time [3,7]. In a cross section of the vessel wall in the x, r plane, because of symmetry, the equations reduce to

$$\rho\frac{\partial^2\xi}{\partial t^2}=\frac{\partial\sigma_{xx}}{\partial x}+\frac{\partial\sigma_{rx}}{\partial r}+\frac{\sigma_{rx}}{r}, \tag{4}$$

$$\rho\frac{\partial^2\eta}{\partial t^2}=\frac{\partial\sigma_{xr}}{\partial x}+\frac{\partial\sigma_{rr}}{\partial r}+\frac{\sigma_{rr}}{r}-\frac{\sigma_{\theta\theta}}{r}. \tag{5}$$

In pulsatile flow, the vessel wall is exposed to two oscillatory forces which provide the input and driving functions for these equations: the shear stress τ_w and pressure p_w acting on the endothelial layer of the vessel wall. In general, these two forces are functions of both time and space (along x). However, the space variations are of the order of magnitude of the propagating wavelength L, which in the systemic circulation at a frequency of 1 Hz is about 10 m. Since a vessel length l is typically much less than L, it has been shown that the space variations can be neglected compared with the time variations in a first approximation [8,7]. The above assumptions are reasonably well satisfied in most of the arterial tree, particularly in the larger more elastic or more muscular arteries, such as the aorta, carotid, iliac, coronary, femoral, celiac, or cerebral arteries. As a first approximation, in this

paper we focus on the oscillations in time which dominate the displacements within the vessel wall and consider a problem in which τ_w and p_w are functions of time only. The x-derivative terms in Eqs. (4) and (5) are thus zero and the two equations become decoupled. In this paper we present solutions in closed form for the displacement ξ and the corresponding stress σ_{rx} of the motion equation in the axial direction,

$$\rho \frac{\partial^2 \xi}{\partial t^2} = \frac{\partial \sigma_{rx}}{\partial r} + \frac{\sigma_{rx}}{r}. \tag{6}$$

Equation (6) represents a problem which is essentially in the x, r plane but with a curvature term σ_{rx}/r arising from the cylindrical polar geometry of the vessel as a whole. It is generally considered that the wall thickness h is one order of magnitude smaller than the vessel radius a [9,7], and since within the vessel wall δr is of order h while r is of order a, it follows that the curvature term in Eq. (6) is an order of magnitude smaller than the other term on the right hand side of the equation and therefore can be neglected, leaving

$$\rho \frac{\partial^2 \xi}{\partial t^2} = \frac{\partial \sigma_{rx}}{\partial r}. \tag{7}$$

A solution of Eq. (6) without this simplification is given in the Appendix for comparison, but this is only possible with certain boundary conditions. A solution of the simplified equation is useful therefore because it can be obtained under more general conditions as we show below, and because it provides a good approximation as is shown in the Appendix.

In order to complete the problem it is necessary to express the stress σ_{rx} in terms of the displacement ξ. It has been shown that linear viscoelastic models provide a good fit of experimental data from the arterial wall [10]. While a generalized nonlinear Maxwell model (a number of Maxwell models linked in parallel) may provide a more accurate fit, this issue has been examined adequately in the past [11,10,4,12] and therefore is not the focus of the present study. Our focus is on the interplay between the elasticity and viscosity of the arterial wall and on obtaining an analytical solution for this purpose.

The relation between the stress σ_{rx} and the corresponding strain ϵ_{rx} for the Maxwell model is given by

$$\frac{\partial \sigma_{rx}}{\partial t} = E\left(\frac{\partial \epsilon_{rx}}{\partial t} - \frac{\sigma_{rx}}{\mu}\right), \tag{8}$$

where E is the modulus of elasticity and μ is the viscosity of the vessel wall. The strain ϵ_{rx} is related to the displacement ξ by

$$\epsilon_{rx} = \frac{\partial \xi}{\partial r} + \frac{\partial \eta}{\partial x}, \tag{9}$$

where the second term on the right hand side is zero on the ground that the imposed shear stress τ_w is taken to be a function of t only, as discussed earlier. Equation (8) then becomes

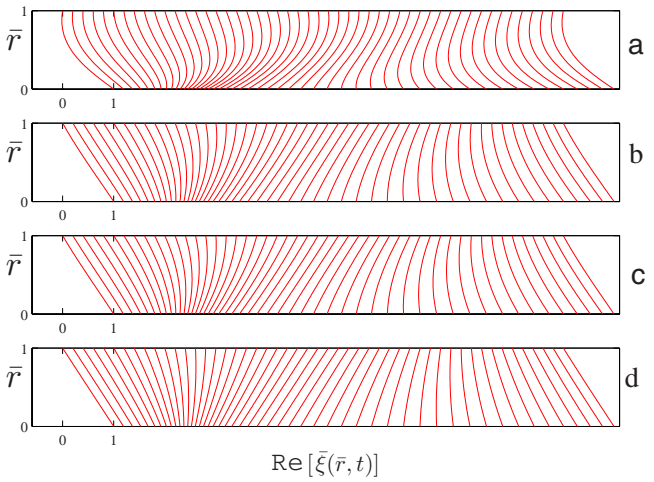

FIG. 1. (Color online) Displacements within the thickness of the vessel wall and within one oscillatory cycle for different degrees of viscoelasticity of the wall material: (a) mostly viscous: $\gamma=0.02$ and $E=E_1=6\times10^6$ dynes/cm [6]; (b) viscoelastic: $\gamma=0.25$ and $E=E_1$; (c) more elastic: $\gamma=1.2$ and $E=E_1$; (d) more rigid: $\gamma=1.2$ and $E=10\times E_1$. The displacement $\bar{\xi}$ and radial coordinate $\bar{r}$ are normalized as shown in Eq. (16). In the real part of the solution (17), the highest displacements occur at time $t=0$.

$$\frac{\partial \sigma_{rx}}{\partial t} = E\frac{\partial^2 \xi}{\partial t \partial r} - \frac{\omega}{\gamma}\sigma_{rx}, \tag{10}$$

where

$$\gamma = \frac{\omega \mu}{E} \tag{11}$$

is a nondimensional parameter which provides a measure of the ratio of viscosity to elasticity within the arterial wall. The extreme values $\gamma=\infty$ and $\gamma=0$ represent a Hookean solid in which elasticity dominates and a Newtonian fluid in which viscosity dominates, respectively [3]. As a point of reference,

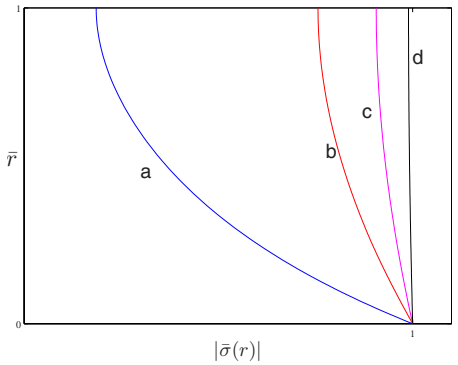

FIG. 2. (Color online) Stress amplitude within the wall thickness and for different degrees of viscoelasticity (a) mostly viscous: $\gamma=0.02$ and $E=E_1=6\times10^6$ dynes/cm^2; (b) viscoelastic: $\gamma=0.25$ and $E=E_1$; (c) more elastic: $\gamma=1.2$ and $E=E_1$ and (d) more rigid: $\gamma=1.2$ and $E=10\times E_1$. $|\bar{\sigma}(r)|$ is the amplitude of the normalized stress defined in Eq. (21) and $\bar{r}$ is normalized radial coordinate defined in Eq. (16). Stress amplitude is greatest in the less viscous and more rigid case.

it has been estimated from experimental results that the value of γ would range between 0.1 and 0.25 in a healthy arterial wall [13–17]. Eliminating the stress between Eqs. (10) and (7), by cross differentiation, finally, yields an equation governing the displacement $\xi(r,t)$ of elements of the vessel wall caused by an oscillatory shear stress $\tau_w(t)$ acting on the endothelial surface:

$$\rho\frac{\partial^3\xi}{\partial t^3} - E\frac{\partial^3\xi}{\partial t\partial r^2} + \frac{\rho\omega}{\gamma}\frac{\partial^2\xi}{\partial t^2} = 0. \tag{12}$$

While the stress σ_{rx} has been eliminated from this equation, the solution for ξ will actually provide a corresponding solution for σ_{rx} and thus provide the stress distribution within the vessel wall as shown in the next section.

III. SOLUTIONS AND RESULTS

A. Bounded case

Here we consider a vessel wall of thickness h, fully tethered at its outer boundary $(r=a+h)$ and subjected to an oscillatory motion at its inner or endothelial boundary $(r=a)$ where a is the vessel radius. Thus the boundary conditions for our problem are

$$\begin{cases} \xi(a,t) = \xi_0 e^{i\omega t} \\ \xi(a+h,t) = 0 \end{cases}, \tag{13}$$

where ω is angular frequency of the imposed oscillatory motion and ξ_0 is its amplitude.

A solution of Eq. (12) with the boundary conditions (13) is of the following form [18]:

$$\xi(r,t) = \frac{e^{\alpha(h-r+a)} - e^{-\alpha(h-r+a)}}{e^{\alpha h} - e^{-\alpha h}}\xi_0 e^{i[\omega t-\beta(r-a)]}, \tag{14}$$

where α and β, after substitution in Eq. (12), are given by

$$\begin{cases} \alpha^2 = \dfrac{\rho\omega^2}{2E}\left[\sqrt{1+\dfrac{1}{\gamma^2}} - 1\right] \\ \beta^2 = \dfrac{\rho\omega^2}{2E}\left[\sqrt{1+\dfrac{1}{\gamma^2}} + 1\right] \end{cases} \tag{15}$$

with $\gamma=\omega\mu/E$ as before. Introducing nondimensional parameters

$$\begin{cases} \bar{r} = (r-a)/h \\ \bar{\xi} = \xi/\xi_0 \\ \Lambda_1 = \alpha h \\ \Lambda_2 = \beta h \end{cases} \tag{16}$$

the solution in nondimensional form becomes

$$\bar{\xi}(r,t) = \frac{e^{\Lambda_1(1-\bar{r})} - e^{-\Lambda_1(1-\bar{r})}}{e^{\Lambda_1} - e^{-\Lambda_1}} e^{i(\omega t-\bar{r}\Lambda_2)} \tag{17}$$

with

$$\begin{cases} \Lambda_1 = \omega h\sqrt{\dfrac{\rho}{2E}\left[\sqrt{1+\dfrac{1}{\gamma^2}} - 1\right]} \\ \Lambda_2 = \omega h\sqrt{\dfrac{\rho}{2E}\left[\sqrt{1+\dfrac{1}{\gamma^2}} + 1\right]} \end{cases}. \tag{18}$$

The real part of the solution (17) corresponds to the real part of the applied displacement, namely $\xi_0\cos(\omega t)$, and the imaginary part corresponds to $\xi_0\sin(\omega t)$. Results for different values of γ and E are shown in Fig. 1.

The stress distribution within the vessel wall can be obtained from Eqs. (7) and (14) as follows:

$$\sigma_{rx}(r,t) = \int_a^r \rho\frac{\partial^2\xi(r,t)}{\partial t^2}dr + \sigma_{rx}(a,t) = \int_a^r \rho\frac{\partial^2}{\partial t^2}\left[\frac{e^{\alpha(h-r+a)} - e^{-\alpha(h-r+a)}}{e^{\alpha h} - e^{-\alpha h}}\xi_0 e^{i[\omega t-\beta(r-a)]}\right]dr + \sigma_{rx}(a,t) =$$

$$-\rho\omega^2\xi_0\int_a^r \frac{e^{\alpha(h-r+a)} - e^{-\alpha(h-r+a)}}{e^{\alpha h} - e^{-\alpha h}}e^{i[\omega t-\beta(r-a)]}dr + \sigma_{rx}(a,t) = \frac{\rho\omega^2\xi_0}{\alpha^2+\beta^2}\frac{(\alpha-i\beta)e^{\alpha(h-r+a)} + (\alpha+i\beta)e^{-\alpha(h-r+a)}}{e^{\alpha h} - e^{-\alpha h}}e^{i[\omega t-\beta(r-a)]}$$

$$= \frac{\xi_0 E}{\sqrt{1+1/\gamma^2}}\frac{(\alpha-i\beta)e^{\alpha(h-r+a)} + (\alpha+i\beta)e^{-\alpha(h-r+a)}}{e^{\alpha h} - e^{-\alpha h}}e^{i[\omega t-\beta(r-a)]}.$$

The stress at the moving boundary $(r=a)$ is given by

$$\sigma_{rx}(a,t) = \frac{\xi_0 E}{\sqrt{1+1/\gamma^2}}\frac{(\alpha-i\beta)e^{\alpha h} + (\alpha+i\beta)e^{-\alpha h}}{e^{\alpha h} - e^{-\alpha h}}e^{i\omega t} \tag{19}$$

which is the highest value of the stress within the wall thickness. This can be put in normalized form

$$\bar{\sigma}_{rx}(\bar{r},t) = \frac{\sigma_{rx}(r,t)}{|\sigma_{rx}(a,t)|} \tag{20}$$

$$= \frac{(\Lambda_1-i\Lambda_2)e^{\Lambda_1(1-\bar{r})} + (\Lambda_1+i\Lambda_2)e^{-\Lambda_1(1-\bar{r})}}{(\Lambda_1-i\Lambda_2)e^{\Lambda_1} + (\Lambda_1+i\Lambda_2)e^{-\Lambda_1}}e^{i(\omega t-\Lambda_2\bar{r})} \tag{21}$$

with $\bar{r}$, Λ_1, and Λ_2 as defined in Eq. (16). The distribution of stress amplitude within the vessel wall is shown in Fig. 2.

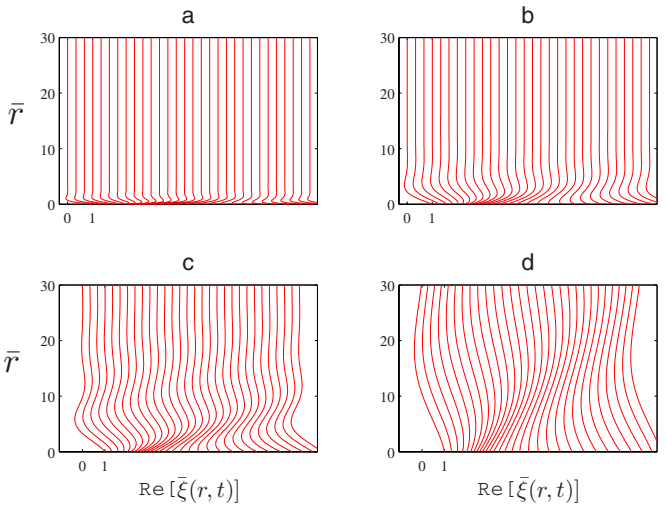

FIG. 3. (Color online) Displacements in an unbounded wall during one oscillatory cycle and for different degrees of viscoelasticity of the wall material: (a) mostly viscous: $\gamma=0.02$ and $E=E_1=6\times10^6$ dynes/cm^2; (b) viscoelastic: $\gamma=0.25$ and $E=E_1$; (c) more elastic: $\gamma=1.2$ and $E=E_1$; (d) more rigid: $\gamma=1.2$ and $E=10\times E_1$. The normalized displacement $\bar{\xi}$ and radial coordinate $\bar{r}$ are defined in Eq. (24). Again, the effect of viscosity is seen to produce an appreciable reduction in the magnitude of the displacement within the wall.

B. Unbounded case

It is of interest to compare the results in the bounded case where the wall is tethered at $r=a+h$ with the purely theoretical case where the wall is tethered at $r=\infty$. We shall refer to this as the "unbounded" case and find that it actually has a useful interpretation as discussed later. The governing equation is the same as before but the boundary conditions are now

$$\begin{cases} \xi(a,t) = \xi_0 e^{i\omega t} \\ \lim_{r\to\infty} \xi(r,t) = 0 \end{cases}, \tag{22}$$

where ω is the angular frequency of the imposed oscillatory motion and ξ_0 is its amplitude.

A solution of Eq. (12) with the boundary conditions (22) is of the following form [18]:

$$\xi(r,t) = \xi_0 e^{-\alpha(r-a)} e^{i[\omega t-\beta(r-a)]}, \tag{23}$$

where α and β are as in Eq. (15). Introducing nondimensional parameters

$$\begin{cases} \bar{r} = (r-a)/a \\ \bar{\xi} = \xi/\xi_0 \\ \Lambda_1 = \alpha a \\ \Lambda_2 = \beta a \end{cases} \tag{24}$$

the solution in nondimensional form becomes

$$\bar{\xi}(r,t) = e^{-\bar{r}\Lambda_1} e^{i(\omega t-\bar{r}\Lambda_2)}. \tag{25}$$

The results are shown in Figs. 3 and 4 where it is seen that the oscillatory displacements imposed at the inner boundary ($r=a$) decay exponentially as they proceed through the wall thickness (see also Eq. (25)). The decay is more rapid (in r) when the wall material is mostly viscous, hence large Λ_1, and the reverse is true when the wall material is less viscous and more rigid.

The stress distribution within the unbounded wall can be determined from the solution for the displacement in Eq. (25),

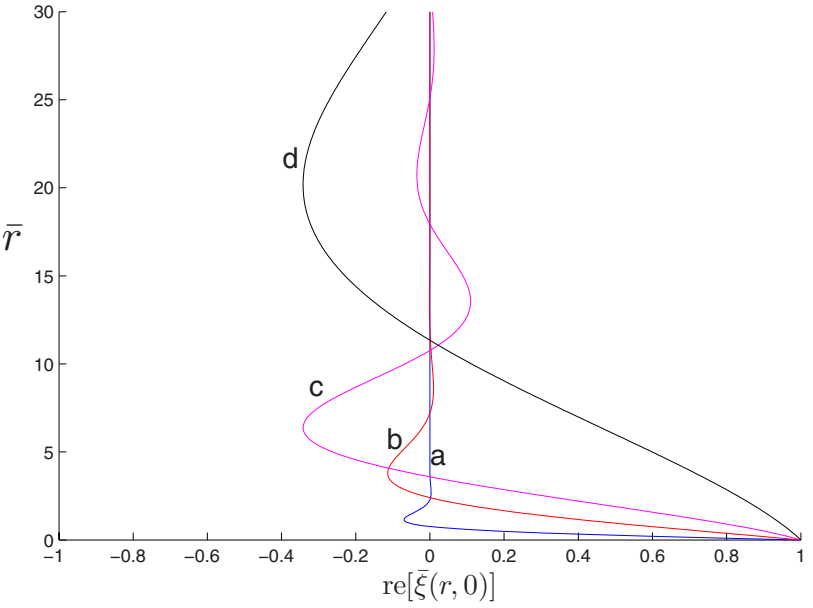

FIG. 4. (Color online) Maximum displacement at different layers of the unbounded wall with different degrees of viscoelasticity of the wall material: (a) mostly viscous: $\gamma=0.02$ and $E=E_1=6\times10^6$ dynes/cm^2; (b) viscoelastic: $\gamma=0.25$ and $E=E_1$; (c) more elastic: $\gamma=1.2$ and $E=E_1$; (d) more rigid: $\gamma=1.2$ and $E=10\times E_1$. The normalized displacement $\bar{\xi}$ and radial coordinate $\bar{r}$ are defined in Eq. (24). Note that in the real part of the solution [Eq. (25)] maximum displacement at the boundary occurs at time $t=0$.

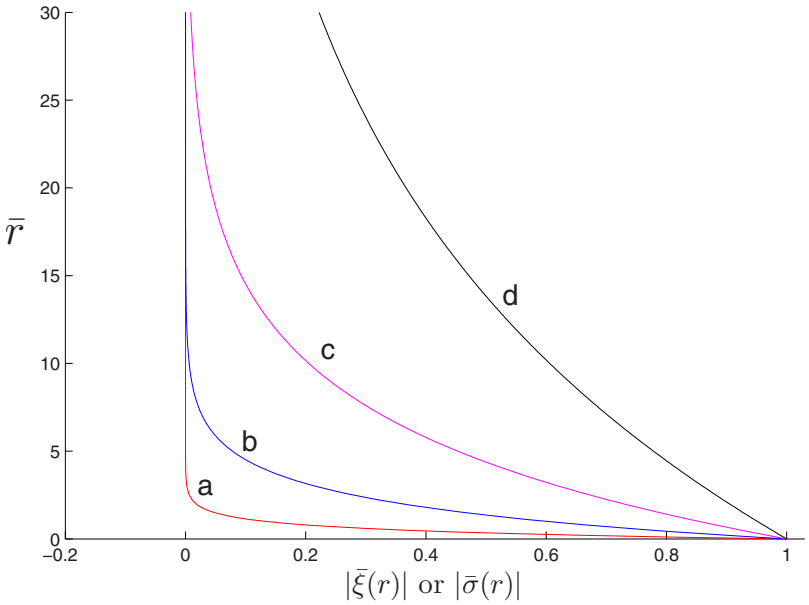

FIG. 5. (Color online) Amplitude of the oscillatory displacement ξ or stress σ_{rx} at different layers of the unbounded wall and for different degrees of viscoelasticity: (a) mostly viscous: $\gamma=0.02$ and $E=E_1=6\times10^6$ dynes/cm^2; (b) viscoelastic: $\gamma=0.25$ and $E=E_1$; (c) more elastic: $\gamma=1.2$ and $E=E_1$; (d) more rigid: $\gamma=1.2$ and $E=10\times E_1$. The normalized displacement $\bar{\xi}(r)$, stress $\bar{\sigma}(r)$, and $\bar{r}$ are defined in Eq. (24). The amplitude is highest in the less viscous and more rigid case.

$$\sigma_{rx}(r,t) = \int_a^r \rho \frac{\partial^2 \xi(r,t)}{\partial t^2} dr + \sigma_{rx}(a,t)$$

$$= \int_a^r \rho \frac{\partial^2}{\partial t^2}[\xi_0 e^{-\alpha(r-a)} e^{i[\omega t - \beta(r-a)]}] dr + \sigma_{rx}(a,t)$$

$$= -\rho\omega^2 \xi_0 \int_a^r e^{-\alpha(r-a)} e^{i[\omega t - \beta(r-a)]} dr + \sigma_{rx}(a,t)$$

$$= \frac{\rho\omega^2 \xi_0 e^{-\alpha(r-a)}}{\alpha + i\beta} e^{i[\omega t - \beta(r-a)]}$$

$$= \frac{(\alpha - i\beta)\xi_0 E}{\sqrt{1+1/\gamma^2}} e^{-\alpha(r-a)} e^{i[\omega t - \beta(r-a)]}. \quad (26)$$

The stress at the moving boundary ($r=a$) is given by

$$\sigma_{rx}(a,t) = \frac{(\alpha - i\beta)\xi_0 E}{\sqrt{1+1/\gamma^2}} e^{i\omega t}. \quad (27)$$

Thus if the stress distribution is nondimensionalized in terms of the stress amplitude at the inner boundary, that is

$$\bar{\sigma}_{rx}(\bar{r},t) = \frac{\sigma_{rx}(r,t)}{|\sigma_{rx}(a,t)|} = e^{-\Lambda_1 \bar{r}} e^{i(\omega t - \Lambda_2 \bar{r})} \quad (28)$$

then the normalized stress distribution will have the same form as the normalized displacement [Eq. (25)]. The results are shown in Fig. 5.

C. Inverse problem: Stress as boundary condition

Results in the previous two sections have shown that if the governing equations and boundary conditions are expressed in terms of *displacement* ξ, then the solution in ξ can ultimately provide the corresponding distribution of stress σ_{rx} within the wall thickness and in particular the stress at the inner boundary ($r=a$) as shown in Eqs. (19) and (27). These results indicate, however, that the stress at the inner boundary as obtained in this way is actually a function of the viscoelastic properties of the wall material through γ. This result means that if we consider the inverse problem whereby the governing equations and boundary conditions are expressed in terms of the stress σ_{rx}, the amplitude of the stress imposed at the inner boundary actually predetermines the viscoelastic properties of the wall material.

Yet, on purely physical grounds, the stress distribution within the wall should be the same whether it is obtained from a problem posed in terms of *displacement* ξ or from one posed in term of stress σ_{rx}. We show below that this is indeed the case.

The governing equation in terms of stress can be obtained by eliminating the displacement ξ between Eqs. (7) and (10) to get

$$\rho \frac{\partial^2 \sigma_{rx}(r,t)}{\partial t^2} - E \frac{\partial^2 \sigma_{rx}(r,t)}{\partial r^2} + \frac{\rho\omega}{\gamma} \frac{\partial \sigma_{rx}(r,t)}{\partial t} = 0. \quad (29)$$

The boundary conditions in terms of the stress are

$$\begin{cases} \sigma_{rx}(a,t) = \sigma_0 e^{i\omega t} \\ \lim_{r\to\infty} \sigma_{rx}(r,t) = 0 \end{cases}, \quad (30)$$

where ω is the angular frequency of the oscillatory stress imposed at the boundary and σ_0 is its amplitude. As in the displacement case, the solution is of the following form:

$$\sigma_{rx}(r,t) = \sigma_0 e^{-\alpha(r-a)} e^{i[\omega t - \beta(r-a)]} \quad (31)$$

with α and β as in Eq. (15). Using the parameters in Eq. (24) the solution in nondimensional form becomes

$$\bar{\sigma}_{rx}(\bar{r},t) = \frac{\sigma_{rx}(r,t)}{\sigma_0} = e^{-\bar{r}\Lambda_1} e^{i(\omega t - \Lambda_2 \bar{r})} \quad (32)$$

which is the same as the nondimensional stress distribution in Eq. (28). Thus, indeed, whether the wall dynamics problem is posed in terms of displacement ξ or stress σ_{rx}, the resulting stress distribution within the wall thickness is the

same *if it is normalized in terms of the stress at the inner boundary* (which is obtained from the displacement solution in one case but is prescribed as a boundary condition in the other).

In the bounded case the problem cannot be prescribed in terms of stress because the stress at the outer boundary is nonzero and is unknown.

D. Maxwell-elastic limit

It is important to verify that the solutions based on the Maxwell-viscoelastic model approach the correct limit as the wall material becomes increasingly less viscous and more elastic. Specifically, we show below that as $\gamma \to \infty$, the solutions obtained in the bounded or the unbounded case [Eqs. (17) and (25)] are the same as those for a purely elastic material.

In a purely elastic material the stress-strain relation is given by Hook's law:

$$\sigma_{rx} = E\epsilon_{rx} = E\frac{\partial \xi}{\partial r}, \tag{33}$$

and the equation for the displacement ξ [using Eq. (7)] then becomes

$$\rho\frac{\partial^2 \xi}{\partial t^2} = E\frac{\partial^2 \xi}{\partial r^2}. \tag{34}$$

This equation together with the boundary conditions (13) provide the solution for the bounded purely elastic case,

$$\bar{\xi}(r,t) = (1-\bar{r})e^{i\omega(t-\bar{r}h\sqrt{\rho/E})}, \tag{35}$$

and together with the boundary conditions (22) give the solution for the unbounded purely elastic case,

$$\bar{\xi}(r,t) = e^{i\omega(t-\bar{r}a\sqrt{\rho/E})}. \tag{36}$$

The bar, as before, refers to nondimensional forms defined in Eqs. (16) and (24).

In our solution for a viscoelastic material the purely elastic limit should be reached as $\gamma \to \infty$. In the bounded case [Eq. (17)] this gives $\Lambda_1 \to 0$, $\Lambda_2 \to \omega h\sqrt{\frac{\rho}{E}}$, and

$$\bar{\xi}(y,t) = (1-\bar{r})e^{i\omega(t-\bar{r}h\sqrt{\rho/E})} \tag{37}$$

which agrees with Eq. (35). In the unbounded case [Eq. (25)] as $\gamma \to \infty$ we find $\Lambda_1 \to 0$, $\Lambda_2 \to \omega a\sqrt{\frac{\rho}{E}}$, and

$$\bar{\xi}(r,t) = e^{i\omega(t-\bar{r}a\sqrt{\rho/E})} \tag{38}$$

which agrees with Eq. (36).

IV. CONCLUSION

Oscillatory shear stress or displacement exerted by pulsatile flow on the endothelial layer of the vessel wall will be transmitted through the wall thickness in a manner which depends critically on the degree of viscoelasticity of the vessel wall and on the degree to which the outer layer of the wall is tethered.

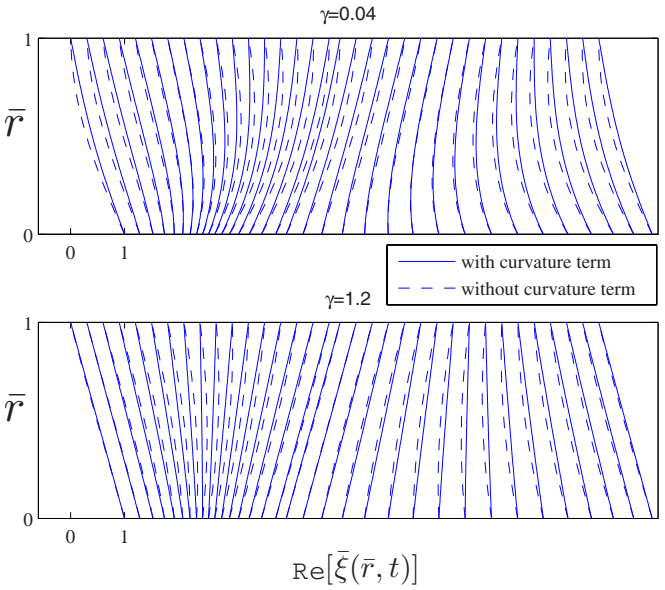

FIG. 6. (Color online) Comparison of results based on Eq. (6) (solid) with those based on the simplified Eq. (7) (dashed), showing displacements within the thickness of the vessel wall and within one oscillatory cycle for different degrees of viscoelasticity of the wall material: (top) mostly viscous: $\gamma=0.04$ and $E=E_1=6\times10^6$ dynes/cm^2, (bottom) more elastic: $\gamma=1.2$ and $E=E_1$. The displacement $\bar{\xi}$ and radial coordinate $\bar{r}$ are normalized as shown in Eq. (A8).

In general, the results show that if the wall material is sufficiently viscous, shear stress and displacements within the wall are confined to a thin layer close to the inner boundary of the wall. As the material of the vessel wall becomes less viscous and more rigid, oscillatory stress and displacements reach deeper into the wall thickness. In particular, if the wall is fully tethered and fairly rigid as may occur in disease or aging [14,16,19,4], the oscillatory stress applied at the endothelial layer is transmitted almost in full magnitude to all layers of the wall. Thus the viscous property of the wall material may be seen as a "protective" element against the axial drag forces of pulsatile flow, while its absence may mark a deterioration in the mechanics of the wall to the effect that the wall becomes less able to withstand the oscillatory forces of pulsatile flow. As a point of reference, it has been estimated from experimental results that the value of γ would range between 0.1 and 0.25 in a healthy arterial wall [13–17].

Pulsatile flow, of course, also exerts radial forces on the vessel wall which in turn lead to circumferential stresses. We have shown that it is possible to decouple these from the axial stresses, which were the main focus of the present paper, by assuming that the shear force exerted by the flow on the endothelial layer is a function of time only, not of the axial coordinate x. This assumption is valid when the length of the propagating flow wave is much larger than the vessel length and has generally been used on these grounds [8,7].

The bounded and unbounded solutions together provide some clues on the issue of tethering. While in both cases the wall is fully tethered at its outer layer, in the unbounded solution the outer layer is at infinity. The unbounded case

may therefore serve as a crude approximation of a vessel wall which has a finite thickness but is not tethered. The results support this approximation reasonably well in that if we focus on only a thin layer of the wall adjacent to the inner boundary of the wall in this case (Fig. 4), the behavior of that layer appears to be what would be expected on physical grounds for a thin wall that is untethered. Specifically, when the material of the untethered wall is highly viscous, the displacement imposed at the inner boundary diminishes rapidly as it is transmitted to the outer boundary even though the outer boundary is free. This would be expected on physical grounds because of the viscous fluidlike wall material in this case. When the material of the untethered wall is less viscous and more rigid, by contrast, the displacement imposed at the inner boundary is transmitted almost in full to the outer boundary and the wall moves "en masse," in this case *because* the outer boundary is free. Again, this would be expected on physical grounds because of the more rigid character of the wall material in this case.

APPENDIX: SOLVING EQ. (6) WITH THE CURVATURE TERM

We show below that the curvature term σ_{rx}/r in Eq. (6), which was neglected because its order of magnitude is lower than that of the other term, has only a small effect on the results. The motion equation [Eq. (6)] together with the stress-strain equation [Eq. (10)] together yield the following equation for the stress:

$$\frac{\partial^2\sigma_{rx}}{\partial r^2}+\frac{1}{r}\frac{\partial\sigma_{rx}}{\partial r}-\frac{\sigma_{rx}}{r^2}-\frac{\rho}{E}\frac{\partial^2\sigma_{rx}}{\partial t^2}-\frac{\rho}{\mu}\frac{\partial\sigma_{rx}}{\partial t}=0. \tag{A1}$$

If we consider the general solution to be $\sigma_{rx}(r,t)=\sigma(r)e^{i\omega t}$ then the general solution for σ is

$$\sigma(r)=AJ_1(\zeta)+BY_1(\zeta), \tag{A2}$$

where J_1, Y_1 are Bessel functions of order one of the first and second kind,

$$\zeta=\frac{\Lambda}{h}r, \tag{A3}$$

$$\Lambda=h\sqrt{\frac{\rho\omega}{\mu}(\gamma-i)}, \tag{A4}$$

and A, B are constants to be determined.

At this stage, we cannot find these constants because the stress at the outer layer of the vessel wall is unknown, but we can calculate the displacement using the general form of the stress,

$$\begin{aligned}\rho\frac{\partial^2\xi}{\partial t^2}&=\frac{\partial\sigma_{rx}}{\partial r}+\frac{\sigma_{rx}}{r}\\&=\frac{\Lambda}{h}\left[A\left(J_0(\zeta)-\frac{1}{\zeta}J_1(\zeta)\right)+B\left(Y_0(\zeta)-\frac{1}{\zeta}Y_1(\zeta)\right)\right.\\&\quad\left.+A\frac{J_1(\zeta)}{r}+B\frac{Y_1(\zeta)}{r}\right]e^{i\omega t}\\&=\frac{\Lambda}{h}[AJ_0(\zeta)+BY_0(\zeta)]e^{i\omega t}.\end{aligned}$$

Integrating twice then yields

$$\xi(r,t)=\frac{-\Lambda}{\rho\omega^2 h}[AJ_0(\zeta)+BY_0(\zeta)]e^{i\omega t}. \tag{A5}$$

To find the constants A and B we now apply the boundary conditions for the displacement [Eq. (13)] and obtain

$$A=\frac{\rho\omega^2 h\xi_0}{\Lambda}\frac{Y_0[\Lambda(a+h)/h]}{J_0[\Lambda(a+h)/h]Y_0[\Lambda(a/h)]-Y_0[\Lambda(a+h)/h]J_0[\Lambda(a/h)]}, \tag{A6}$$

$$B=-\frac{\rho\omega^2 h\xi_0}{\Lambda}\frac{J_0[\Lambda(a+h)/h]}{J_0[\Lambda(a+h)/h]Y_0[\Lambda(a/h)]-Y_0[\Lambda(a+h)/h]J_0[\Lambda(a/h)]}. \tag{A7}$$

Using the nondimensional parameters

$$\begin{cases}\bar{a}=a/h\\ \bar{r}=(r-a)/h\\ \bar{\xi}=\xi/\xi_0\\ \Lambda=h\sqrt{\dfrac{\rho\omega}{\mu}(\gamma-i)}\end{cases} \tag{A8}$$

the normalized displacement is then given by

$$\bar{\xi}(r,t)=-\frac{J_0[\Lambda(1+\bar{a})]Y_0[\Lambda(\bar{r}+\bar{a})]-Y_0[\Lambda(1+\bar{a})]J_0[\Lambda(\bar{r}+\bar{a})]}{J_0[\Lambda(1+\bar{a})]Y_0(\Lambda\bar{a})-Y_0[\Lambda(1+\bar{a})]J_0(\Lambda\bar{a})}e^{i\omega t}. \tag{A9}$$

Figure 6 shows the results from Eq. (A9) above, which is based on Eq. (6), compared with the results obtained earlier based on the simplified Eq. (7) in which the curvature term was neglected. It is seen that the differences between the two are very small, therefore the simplified problem based on Eq. (7) provides a good approximation.

[1] M. Cinthio, A. R. Ahlgren, J. Bergkvist, T. Jansson, H. W. Persson, and K. Lindstrom, Am. J. Phys. **291**, 394 (2006).

[2] M. Persson, A. R. Ahlgren, T. Jansson, A. Eriksson, H. W. Persson, and K. Lindstrom, Clin. Imaging **23**(5), 247 (2003).

[3] R. Darbey, *Viscoelastic Fluids* (Marcel Dekker Inc., New York, 1976).

[4] G. A. Holzapfel, T. C. Gasser, and M. Stadler, Eur. J. Mech. A/Solids **21**, 441 (2002).

[5] W. W. Nichols and M. F. O'Rourke, *McDonald's Blood Flow in Arteries: Theoretical, Experimental and Clinical Principles* (Edward Arnold, London, 2005).

[6] J. C. Lasheras, Annu. Rev. Fluid Mech. **39**, 293 (2007).

[7] M. Zamir, *The Physics of Pulsatile Flow* (Springer-Verlag, New York 2000).

[8] J. R. Womersley, Wright Air Development Center Technical Report, WADC-TR 56–614, 1957 (unpublished).

[9] D. A. McDonald, *Blood Flow in Arteries*, 2nd ed.(Williams and Wilkins, Baltimore, 1974).

[10] M. Orosz, G. Molnarka, M. Toth, G. L. Nadasy, and E. Monos, Med. Sci. Monit. **5**, 549 (1999).

[11] W. R. Milnor, *Hemodynamics* (Williams and Wilkins, Baltimore, 1982).

[12] R. Vito and S. Dixon, Annu. Rev. Biomed. Eng. **5**, 413 (2003).

[13] D. H. Bergel, J. Physiol. (London) **156**, 458 (1961).

[14] B. M. Learoyd and M. G. Taylor, Circ. Res. **18**, 278 (1966).

[15] R. H. Cox, Am. J. Physiol. Heart Circ. Physiol. **246**, H90 (1984).

[16] W. Band, W. J. A. Goedhard, and A. A. Knoop, Pfluegers Arch. **331**, 357 (1971).

[17] D. H. Bergel, *Cardiovascular Fluid Dynamics* (Academic, London, 1972), Vol. 2.

[18] H. Kolsky, *Stress Waves in Solids* (Dover Publication, New York, 1963).

[19] A. Simon and J. Levenson, Am. J. Hypertens. **8**, 45S (1995).